Electrochemistry and Electrogenerated Chemiluminescence of All-trans Conjugated Polymer Poly[distyrylbenzene-*b*-(ethylene Oxide)]s

Dale J. Rosado, Jr. and Wujian Miao*

Department of Chemistry and Biochemistry, The University of Southern Mississippi, Box 5043, Hattiesburg, Mississippi 39406

Qunhui Sun and Yulin Deng

School of Chemical and Biomolecular Engineering and IPST at GT, Georgia Institute of Technology, Atlanta, Georgia 30332-0620

Received: May 1, 2006; In Final Form: June 13, 2006

The electrochemistry and electrogenerated chemiluminescence (ECL) of two linear, stereoregular, and structurally defined PPV derivatives, poly[distyrylbenzene-*b*-(ethylene oxide)]s, with respective 12 and 16 of ethylene oxide repeat units in the backbone, abbreviated as DE−1 and DE−2, have been studied on glassy carbon and Pt electrodes in CH_2Cl_2 and CH_3CN containing 0.10 M tetra-*n*-butylammonium perchlorate (TBAP). In CH_2Cl_2, a one-electron transfer, reversible oxidation at ∼0.75 V vs Ag/Ag^+ (10 mM $AgNO_3$ in CH_3CN) was observed for both polymers. Porous polymer films were electrochemically formed on the electrode with multiple cyclic potential scanning. Cast films of DE−1 and DE−2 on the electrode prepared from 1.0 mM of the corresponding CH_2Cl_2 solutions were used for studies in CH_3CN containing 0.10 M TBAP due to their limited solubility in the solvent. A film-type of oxidation was found at ∼0.80 V vs Ag/Ag^+ in CH_3CN when a scan rate of less than 1 V/s was used. The soluble oxidation product can be captured and reduced and then reoxidized in solution-phase at the electrode at a relatively high scan rate of, e.g., 2 V/s. ECL responses with a maximum emission at ∼1.10 V vs Ag/Ag^+ were obtained with the cast films in CH_3CN (0.10 M TBAP) in the presence of 43 mM tri-*n*-propylamine (TPrA) after both TPrA and film were oxidized. The ECL is believed to be resulted from the interaction between the oxidized polymer species and the strong reducing TPrA free radical ($TPrA^{\bullet}$) generated after the deprotonation of $TPrA^{\bullet+}$ cation species.

Introduction

Electrogenerated chemiluminescence (or electrochemiluminescence, ECL)[1] is a process of light generation without heat by electrical excitation.[2] ECL studies of conjugated polymers,[3−10] such as poly(*p*-phenylene vinylene) (PPV)[11] and its derivatives MEH−PPV,[12−16] BuEH−PPV,[17] DB−PPV,[18] and "OC1C10" PPV,[19−21] have drawn much attention for potential applications in a new generation of large flat-panel displays[22−24] since the first ECL report of PPV was published in 1990.[11] There are basically four different types of conjugated polymer-based ECL configurations in the literature. The first one involves a thin layer of conjugated polymer (∼100 nm in thickness) sandwiched between a metal layer and a transparent ITO electrode.[5] After the injection of electrons and holes from negative and positive electrodes, respectively, electrons and holes capture one another within the polymer film and form neutral bound excited states that emit light. Instead of solid-state polymer thin layer, the second type of polymer-ECL configuration uses a polymer solution or gel (∼1−2 μm) sandwiched between two ITO electrodes as the light-emitting medium.[25−29] The third one uses only one working electrode such as Pt coated with a thin polymer film in contact with an electrolyte solution.[13,15,18] By application of alternating anodic and cathodic potential steps, positive and negative polarons are produced in the polymer, and the annihilation reaction results in ECL transients. The forth type of polymer-ECL configuration is obtained on the basis of the third one with addition of an ECL coreactant such as tri-*n*-propylamine (TPrA) or persulfate species into the electrolyte solution.[15] In this case, only one direction of potential scanning, either positive or negative, is needed for the production of ECL. A common requirement for the first three polymer-ECL configurations is that the studied polymer must be oxidized as well as reduced under the experimental conditions, which, in some cases, is difficult to meet. For example, the potential window of the solvent used may be smaller than that for the polymer oxidation or reduction, or simply the polymer cannot be oxidized and also reduced. As a result, coreactant ECL provides an excellent alternative way for the ECL production of such conjugated polymers.

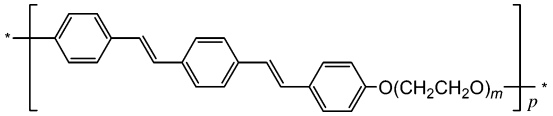

Figure 1. Molecular structure of poly[distyrylbenzene-*b*-(ethylene oxide)]s. Short names of DE−1 and DE−2 were used for $m = 12$, $p = 6$ (MW = 4943 g/mole), and for $m = 16$, $p = 8$ (MW = 7952 g/mole), respectively.[31]

The excitons generated electrically are believed to be the same as those generated by photoexcitation.[8,30] Thus, an ideal polymer

* To whom correspondence should be addressed. Tel: +1 601-266 4716; Fax: +1 601-266 6075; E-mail: wujian.miao@usm.edu.

10.1021/jp062650g CCC: $33.50
Published on Web 07/25/2006

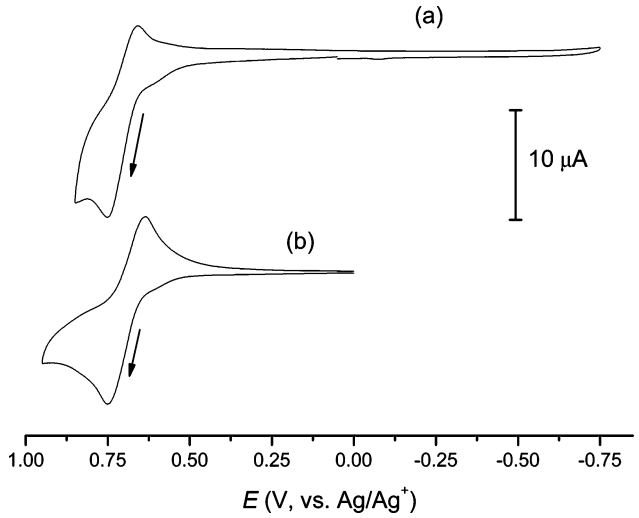

Figure 2. Cyclic voltammograms obtained from (a) 1.0 mM DE−1 and (b) 1.0 M DE−2 in CH_2Cl_2 containing 0.10 M TBAP at a 3 mm in diameter GC electrode with a scan rate of 50 mV/s.

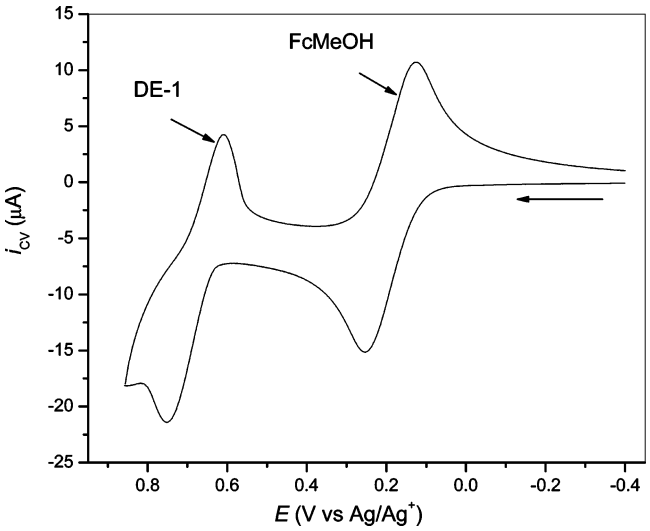

Figure 3. Cyclic voltammogram obtained from 1.0 mM DE−1 −1.0 mM FcMeOH in CH_2Cl_2 containing 0.10 M TBAP at a 3 mm in diameter GC electrode with a scan rate of 50 mV/s. Potential scanning range used: −0.40−0.85 V vs Ag/Ag^+.

used in polymer-ECL device must possess high photoluminescence (PL) quantum efficiency. Recently, two linear, stereoregular, and structurally defined PPV derivatives, poly-[distyrylbenzene-*b*-(ethylene oxide)]s, with respective 12 and 16 of ethylene oxide repeat units in the backbone, abbreviated as DE−1 and DE−2, have been synthesized[31] (Figure 1). A high photoluminescence quantum yield (PLQY) of 85% for both DE−1 and DE−2 in dichloromethane (CH_2Cl_2) and an even higher PLQY of 96% in MeOH−CH_2Cl_2 mixture (40:60 in v/v) for DE−1 were obtained.[31] In this report, the electrochemical behavior of solution phase DE−1 and DE−2 in CH_2Cl_2 at glassy carbon (GC) electrode and cast films DE−1 and DE−2 on Pt electrode in acetonitrile (CH_3CN) was presented, followed by the coreactant ECL studies of cast films DE−1 and DE−2 on Pt in CH_3CN in the presence of coreactant TPrA.

Experimental Section

Chemicals. Dichloromethane (DCM, CH_2Cl_2, spectroscopy grade 99.9%) from Fisher Scientific (Fairlawn, NJ), acetonitrile (CH_3CN, HPLC grade 99.93+ %), ferrocene methanol (FcMeOH, 97%), and tri-*n*-propylamine (TPrA, 99+%) from Sigma-Aldrich (Milwaukee, WI), silver nitrate ($AgNO_3$, 99.5%), and tetra-*n*-butylammonium perchlorate (TBAP, electrochemical grade) from Fluka (Milwaukee, WI), and poly[distyrlbenzene-*b*-(ethylene oxide)]s (DE−1 and DE−2) from Georgia Institute of Technology (Atlanta, GA) were used as received.

Electrochemical, ECL, and Fluorescent Measurements. Cyclic voltammetry (CV) was performed with a model 660A electrochemical workstation (CH Instruments, Austin, TX). A conventional three-electrode cell was used, with a Pt wire as the counter electrode and an Ag/Ag^+ (10 mM $AgNO_3$ in 0.10 M TBAP CH_3CN) as the reference electrode. FcMeOH/$FcMeOH^+$ couple was used as an internal potential standard and had a half-wave potential of 0.19 V vs Ag/Ag^+ in CH_2Cl_2 (0.10 M TBAP). Two different types of working electrodes, namely 3-mm in diameter glassy carbon (GC) and 2-mm in diameter Pt, were used for solution-phase DE−1 and DE−2 dissolved in DCM (electrolyte) and for DE−1 and DE−2 cast-films in contact with CH_3CN (electrolyte) electrochemical (CV and ECL) measurements, respectively. The cast-film was prepared by dispersing a 10 μL droplet of 1.0 mM DE−1 or DE−2 DCM solution onto the Pt electrode disk, where the CH_2Cl_2 solvent was allowed to be evaporated in the air for ∼3−5 min. The ECL along with the CV signals were measured simultaneously with the 660A electrochemical workstation (see above) combined with a photomultiplier tube (PMT, Hamamatsu R928, Japan) installed under the electrochemical cell. A voltage of −700 V was supplied to the PMT with a high voltage power supply (Model 472A Brandenburg PMT power supply, England). The light signal (as photocurrent) was detected with a high sensitive Keithley 6514 electrometer (Keithley, Cleveland, OH) and converted to a voltage (in ± 2V) that was connected to the electrochemical workstation computer. Fluorescence spectra were recorded with a Spex Fluorolog 2 fluorimeter (Horiba Jobin Yvon Inc., NJ).

All measurements were conducted at a temperature of 20 ± 2 °C, unless otherwise stated.

Results and Discussion

Electrochemistry of DE−1 and DE−2 in CH_2Cl_2. Because DE−1 and DE−2 are completely soluble in CH_2Cl_2[31] but sparely soluble in CH_3CN, their electrochemical studies were first conducted in CH_2Cl_2 containing 0.10 M TBAP electrolyte. As shown in Figure 2, very similar and well-defined reversible redox waves are obtained for both DE−1 (Figure 2a) and DE−2 (Figure 2b), with the oxidation peak potentials at ∼0.75 V vs Ag/Ag^+ and the rereduction peak potentials at ∼0.62 V vs Ag/Ag^+. No reduction was found for DE−1 and DE−2 under the experimental conditions presently used. Because the electrochemical as well as ECL behavior (see below) of DE−1 and DE−2 is very close, in the rest of the report, only experimental data from DE−1 will be presented and discussed unless otherwise stated. To verify the reversibility and to estimate the number of electron transfers involved in the redox process of DE−1, a well-known fully reversible, one electron-transfer species FcMeOH with a final concentration of 1.0 mM was added into 1.0 mM DE−1 CH_2Cl_2 solution. Note that Fc can be also used and similar results are expected to be obtained. Figure 3 shows the cyclic voltammogram of such a solution using 3 mm in diameter GC electrode at a scan rate of 50 mV/s. A peak potential separation of 135 mV vs 129 mV and a peak-to-peak current of 25 vs 26 μA are obtained from Figure 3 for species DE−1 vs FcMeOH, respectively. This suggests that the redox reaction of DE−1 is a fully reversible, one electron-transfer process. As will be discussed below, however,

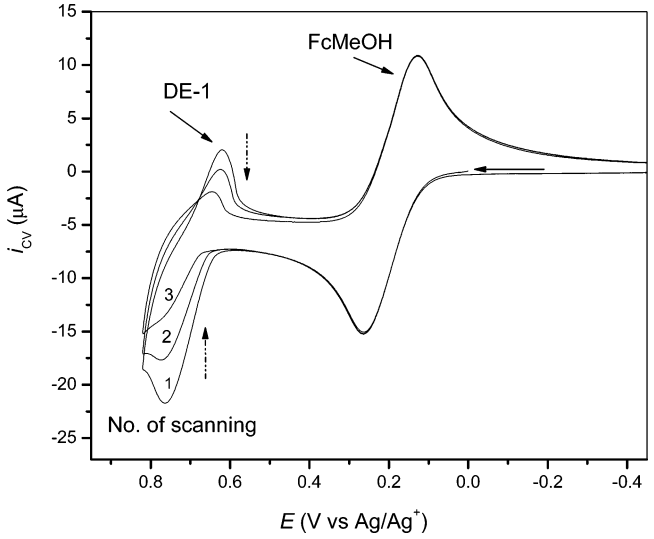

Figure 4. Multiple scan cyclic voltammograms obtained from 1.0 mM DE−1−1.0 mM FcMeOH in CH_2Cl_2 containing 0.10 M TBAP at a 3 mm in diameter GC electrode with a scan rate of 50 mV/s. Potential scanning range used: −0.45−0.80 V vs Ag/Ag^+.

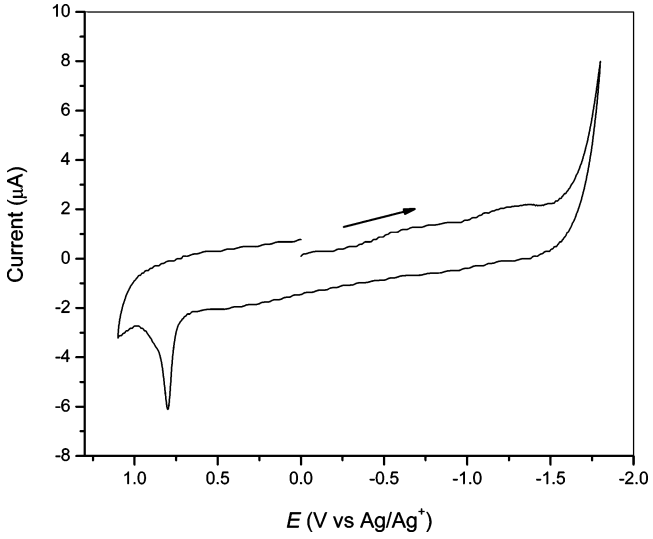

Figure 5. Cyclic voltammogram of DE−1 cast film on 2-mm in diameter Pt electrode placed in CH_3CN containing 0.10 M TBAP. Scan rate = 100 mV/s. The cast film was produced using 10 μL of 1.0 mM DE−1 CH_2Cl_2 solution.

this reversible process involves weak adsorptions. Consequently, the present electrode reactions cannot be regarded as classical diffusion-controlled Nernstian electron-transfer reactions. The large peak potential separation with respective to the theoretical value of 56/*n* mV at 20 °C[32] (for FcMeOH, $n = 1$) is due to the uncompensated ohmic *iR* drop, which has been frequently observed in high resistance organic solvents[33] such as CH_2Cl_2 in the present study. Not surprisingly, the peak potential separations were found to be increased slightly with the increase of scan rate. For example, at a scan rate of 125 mV/s, FcMeOH and DE−1 showed peak separation values of 161 and 163 mV, respectively. The similar peak potential separation values of these two species under different scan rates confirm that the electron transfer of DE−1 at GC electrode is comparably fast.

Close examination of the relationship between the anodic peak current and the square root of the scan rate finds that weak adsorption of DE−1 polymer on GC electrode occurred, because at relatively high scan rates, the anodic peak current vs $v^{1/2}$ deviates from the straight line and increases rapidly. (See Figure S1 in Supporting Information). Electrochemical polymerization of DE−1 at GC electrode occurred during multiple cyclic potential scanning (Figure 4). With the increase of the scan number, redox currents gradually decrease, suggesting that the film formed at the electrode is not conductive. No change is found in FcMeOH electrochemical behavior, implying that the electrochemically produced film is porous so that relatively small FcMeOH molecules can freely diffuse within the polymer film. The produced polymer film can be easily observed under a UV light and showed a maximum fluorescent emission at ∼430 nm (See Figure S2 in Supporting Information). The emission behavior of the polymer film is close to that of DE−1 dissolved in organic solvents such as CH_2Cl_2 and MeOH−CH_2Cl_2 mixtures in which two maximum emission peaks at ∼410 nm and ∼430 nm were observed.[31]

Similar electrochemical behavior of DE−1 and DE−2 was observed in CH_2Cl_2 when a 2-mm in diameter Pt disk electrode was used as the working electrode.

Electrochemistry of DE−1 Cast Film on Pt in CH_3CN. Because no ECL was found in CH_2Cl_2, we decided to study the electrochemical and ECL behavior (see below) of cast film DE−1 in CH_3CN, in which the solubility of DE−1 is insignificant. Also, since in CH_3CN the ECL intensity produced at

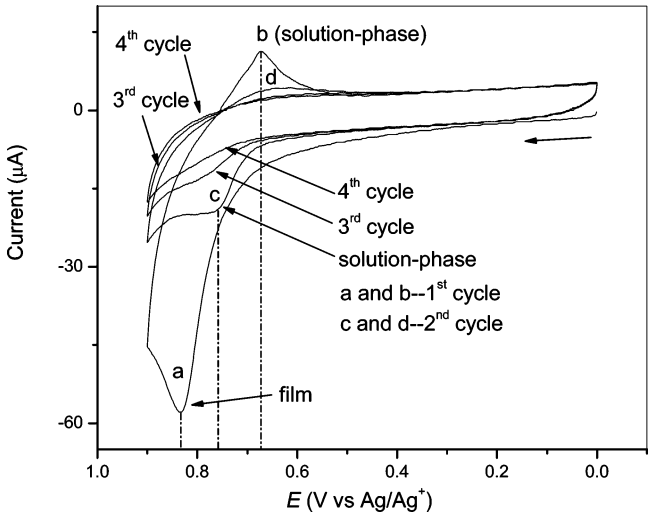

Figure 6. Cyclic voltammograms of DE−1 cast film on 2-mm in diameter Pt electrode placed in CH_3CN containing 0.10 M TBAP at a high scan rate of 2 V/s. The cast film was produced using 10 μL of 1.0 mM DE−1 CH_2Cl_2 solution. See main text for the explanation of notation a−d.

Pt electrode generally larger than that obtained from GC,[34] a 2-mm in diameter Pt was chosen as the working electrode in the studies reported here. As shown in Figure 5, a characteristic film-like oxidation peak at ∼0.80 V vs Ag/Ag^+ is observed for DE−1 cast film on Pt at a scan rate of 100 mV/s. Neither peak on reversal scan nor reduction of DE−1 in CH_3CN is found under the present experimental conditions. This is because in this time scale, the soluble oxidation product was completely diffused away from the electrode surface into the bulk electrolyte solution. In contrast, at high potential scan rates (> 1 V/s), both solid-state and solution-phase redox processes can be observed. For example, at a scan rate of 2 V/s (Figure 6), after the film oxidation at ∼0.83 V vs Ag/Ag^+ (peak a), the soluble product is captured and rereduced at ∼0.67 V vs Ag/Ag^+ (peak b). The second cycle of the cyclic voltammetry shows the pure solution-phase redox behavior of DE−1 in CH_3CN (peaks c and d). Similar phenomena were reported previously for solid-state C_{60} reduction in DCM.[35] On the basis of the theory presented in that paper, it is predicted that the solid film should be oxidized

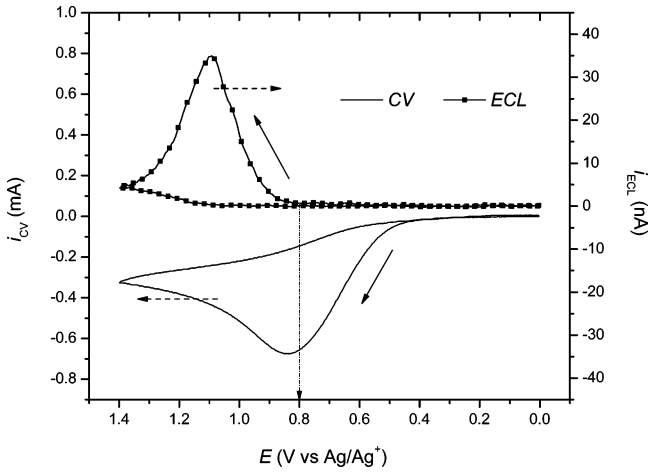

Figure 7. CV and ECL of cast film DE−1 on 2-mm in diameter Pt placed in 0.10 M TBAP CH_3CN containing 43 mM TPrA. Scan rate used: 100 mV/s.

at more positive potentials with respect to the oxidation of solution-phase species, which is consistent with the experimental results shown in Figure 6. During the polymer film redox process, "break-in" phenomenon associated with film solvation and ion-incorpotion processes could be also involved.

Electrogenerated Chemiluminescence of DE−1 and DE−2. Because DE−1 and DE−2 can only be oxidized but not reduced in CH_2Cl_2 and CH_3CN (Figures 2−6), their ECL cannot be produced by annihilation. As a result, ECL behavior of DE−1 and DE−2 were investigated by using coreactant ECL.[36] Although several coreactants such as TPrA and oxalate could be used along with oxidizable fluorophore molecules to produce ECL signals upon anodic potential scanning, it has been found that TPrA generally gives the studied system the highest ECL efficiencies.[36] We used TPrA with a variety of concentrations as the coreactant for solution-phase DE−1 and DE−2 ECL studies in CH_2Cl_2. Surprisingly, no ECL was found in all cases, indicating that TPrA cation and free radicals produced after its oxidation are probably not stable in CH_2Cl_2. In CH_3CN, however, ECL was observed for cast film DE−1 or DE−2 on Pt placed in 0.10 M TBAP CH_3CN in the presence of coreactant TPrA upon the oxidation of TPrA and DE−1 or DE−2. As shown in Figure 7, when electrode potential is scanned from 0 to 1.4 V vs Ag/Ag^+, TPrA starts to oxidize at ~0.5 V and forms a large oxidation peak at ~0.84 V vs Ag/Ag^+. The ECL signal, however, starts to arise at potential of 0.80 V vs Ag/Ag^+, which is corresponding to the oxidation of cast film DE−1 on Pt in CH_3CN (Figure 5). The ECL shows a maximum value of ~35 nA at 1.10 V vs Ag/Ag^+. No ECL was observed on the following potential cycling although the CV profile was similar to the initial one (not shown). This can be readily explained, because after the first potential cycle, the cast film of DE−1 on Pt electrode is oxidized to form soluble species that diffuse away from the electrode and react with radicals generated from TPrA oxidation to form ECL signals. As for CV, although cast film DE−1 is oxidized during the first potential cycle, its contribution to the overall electrode current is negligible (see Figure 5 vs Figure 7).

The ECL intensity-coreactant TPrA concentration profile indicates that ECL has a maximum value at [TPrA] ≈ 43 mM (Figure 8). Higher TPrA concentrations than 43 mM may cause the dissolution of cast film DE−1 at the electrode, via, e.g., hydrophobic interactions between TPrA and the polymer film, hence decreasing the ECL intensity.

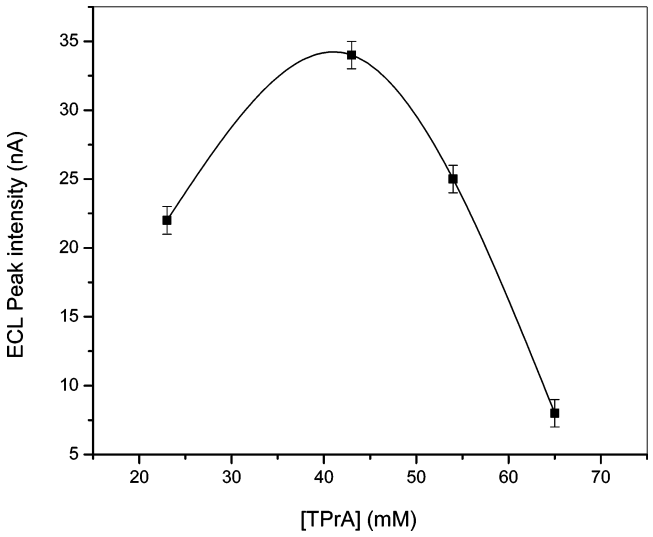

Figure 8. ECL intensity of cast film DE−1 on Pt in 0.10 M TBAP CH_3CN as a function of coreactant TPrA concentration. Scan rate used: 100 mV/s.

Compared to DE−1, very similar coreactant ECL behavior of cast film DE−2 on Pt in CH_3CN was observed (not shown), which is expected, since as described earlier, both DE−1 and DE−2 showed similar electrochemical behavior.

On the basis of the CV and coreactant ECL features of cast film DE−1 in CH_3CN, the relevant ECL mechanism can be proposed as follows (Scheme 1):[15,36]

SCHEME 1: ECL Mechanism of Cast Film DE−1 on Pt in CH_3CN with TPrA as Coreactant

$$\text{TPrA} \xrightarrow{-e} \text{TPrA}^{\bullet+} \xrightarrow{-H^+} \text{TPrA}^{\bullet}$$

$$\text{DE-1(film)} \xrightarrow{-e} \{[\text{DE-1}]^+(\text{film})\} \longrightarrow [\text{DE-1}]^+(\text{soln})$$

$$[\text{DE-1}]^+(\text{soln}) + \text{TPrA}^{\bullet} \longrightarrow [\text{DE-1}]^*(\text{soln}) + \text{P}$$

$$[\text{DE-1}]^*(\text{soln}) \longrightarrow \text{DE-1(soln)} + h\nu$$

$$(\text{Where P} = Pr_2N^+HC{=}CH_2CH_3)$$

Coreactant TPrA oxidizes to form $TPrA^{\bullet+}$ cation radical which immediately deprotonates to form $TPrA^{\bullet}$ free radical. When the electrode potential reaches the oxidation potential of DE−1, DE−1 film oxidizes to form solution-phase $[DE-1]^+$ cation radical. When $TPrA^{\bullet}$ free radical diffuses away from the electrode and meets $[DE-1]^+$ cation radical, the excited state [DE−1]* is formed after an electron-transfer process. Finally, the ECL is observed after [DE−1]* emits photons and returns to ground-state DE−1.

Although we have not been able to get the ECL spectrum of DE−1-TPrA system, mainly because of the instability of the

SCHEME 2: Schematic Energy Diagram Showing the ECL Formation After the Anodic Oxidation of DE−1 and TPrA

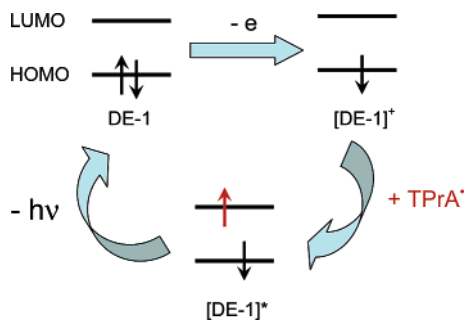

ECL production from DE−1 film in CH_3CN, on the basis of the energy diagram (Scheme 2), we could predict the ECL spectrum is in the visible spectrum range. Because $E^{a}_{DE-1} \approx 0.80$ V vs Ag/Ag^+ (Figure 5), and $E^{0}_{TPrA\bullet} \approx -1.7$ V vs SCE,[37] the energy gap between the excited state and the ground state for DE−1 is estimated to be ∼2.5 V, which corresponds to $\pi^* \rightarrow \pi$ bonding transitions[15,31] and has the emission wavelength of ∼490 nm. This, of course, is only an estimation, and the real ECL spectrum would be similar to that obtained from photoemissions with a maximum peak around 430 nm.[31]

Conclusions

Conjugated polymers DE−1 and DE−2 showed one electron transfer, reversible oxidation waves in CH_2Cl_2 (0.10 M TBAP) at GC electrode, with the oxidation peak potentials at ∼0.75 V vs Ag/Ag^+ and the rereduction peak potentials at ∼0.62 V vs Ag/Ag^+. Upon multiple anodic potential scanning, nonconductive porous films were produced at the electrode. In CH_3CN at relatively fast scan rates of > 1 V/s, solid- and solution-phase chemically reversible oxidation waves of DE−1 (DE−2) cast film on Pt was observed. Such cast films can generate ECL signals with a maximum emission at ∼1.10 V vs Ag/Ag^+ upon the anodic potential scanning from 0 to 1.40 V vs Ag/Ag^+ in CH_3CN (0.10 M TBAP) in the presence of coreactant TPrA.

Acknowledgment. Financial support from USM startup, USM CoST DRI grant, NSF-MRSEC (USM) program, and NSF-OISE−0535467 is gratefully acknowledged.

Supporting Information Available: The relationship between the anodic peak current and the square root of the scan rate obtained from 1.0 mM DE−1 at a 3 mm in diameter GC electrode, an image of electrochemically formed polymer film on GC electrode under UV light, and the fluoresence spectrum of the polymer film are available in the SI. This material is available free of charge via the Internet at http://pubs.acs.org.

References and Notes

(1) Note: Although "electroluminescence (EL)" has been widely used in the literature, the light-emitting mechanism is believed to be the same or very similar to that described by electrogenerated chemiluminescence or electrochemiluminescence (ECL). As a result, term "ECL" is used throughout this report.

(2) Bard, A. J., Ed. *Electrogenerated Chemiluminescence*; Marcel Dekker: New York, 2004.

(3) Armstrong, N. R.; Wightman, R. M.; Gross, E. M. *Annu. Rev. Phys. Chem.* **2001**, *52*, 391−422.

(4) Buda, M. In *Electrogenerated Chemiluminescence*; Bard, A. J., Ed.; Marcel Dekker: New York, 2004; Chapter 10.

(5) Friend, R. H.; Gymer, R. W.; Holmes, A. B.; Burroughes, J. H.; Marks, R. N.; Taliani, C.; Bradley, D. D. C.; Dos Santos, D. A.; Bredas, J. L.; Logdlund, M.; Salaneck, W. R. *Nature* **1999**, *397*, 121−128.

(6) Greenham, N. C.; Friend, R. H. *Solid State Phys.* **1995**, *49*, 1−149.

(7) Kalinowski, J. *J. Phys. D: Appl. Phys.* **1999**, *32*, R179−R250.

(8) Kraft, A.; Grimsdale, A. C.; Holmes, A. B. *Angew. Chem., Int. Ed.* **1998**, *37*, 403−428.

(9) Mitschke, U.; Bauerle, P. *J. Mater. Chem.* **2000**, *10*, 1471−1507.

(10) Patel, N. K.; Cina, S.; Burroughes, J. H. *IEEE J. Selected Topics in Quan. Electron.* **2002**, *8*, 346−361.

(11) Burroughes, J. H.; Bradley, D. D. C.; Brown, A. R.; Marks, R. N.; Mackay, K.; Friend, R. H.; Burns, P. L.; Holmes, A. B. *Nature* **1990**, *347*, 539−541.

(12) Dini, D.; Martin, R. E.; Holmes, A. B. *Ad. Funct. Mater.* **2002**, *12*, 299−306.

(13) Janakiraman, U.; Dini, D.; Preusser, A.; Holmes, A. B.; Martin, R. E.; Doblhofer, K. *Synth. Met.* **2001**, *121*, 1685−1686.

(14) Chang, S.-C.; Li, Y.; Yang, Y. *J. Phys. Chem. B* **2000**, *104*, 11650−11655.

(15) Richter, M. M.; Fan, F.-R. F.; Klavetter, F.; Heeger, A. J.; Bard, A. J. *Chem. Phys. Lett.* **1994**, *226*, 115−120.

(16) Pei, Q.; Yu, G.; Zhang, C.; Yang, Y.; Heeger, A. J. *Science* **1995**, *270*, 719.

(17) Yu, G.; Cao, Y.; Andersson, M.; Gao, J.; Heeger, A. J. *Adv. Mater.* **1998**, *10*, 385−388.

(18) Janakiraman, U.; Doblhofer, K.; Fischmeister, C.; Holmes, A. B. *J. Phys. Chem. B* **2004**, *108*, 14368−14373.

(19) Andersson, G. G.; Gommans, H. H. P.; Denier Van Der Gon, A. W.; Brongersma, H. H. *J. Appl. Phys.* **2003**, *93*, 3299−3307.

(20) Andersson, G. G.; de Jong, M. P.; Janssen, F. J. J.; Sturm, J. M.; van Ijzendoorn, L. J.; Denier van der Gon, A. W.; de Voigt, M. J. A.; Brongersma, H. H. *J. Appl. Phys.* **2001**, *90*, 1376−1382.

(21) Andersson, G. G.; de Jong, M. P.; van Ijzendoorn, L. J.; Denier van der Gon, A. W.; Brongersma, H. H.; de Voigt, M. J. A. *Synth. Met.* **2001**, *121*, 1675−1676.

(22) Mikroyannidis, J. A.; Spiliopoulos, I. K.; Kasimis, T. S.; Kulkarni, A. P.; Jenekhe, S. A. *J. Polym. Sci. Part A: Polym. Chem.* **2004**, *42*, 2112−2123.

(23) Sheats, J. R.; Antoniadis, H.; Hueschen, M.; Leonard, W.; Miller, J.; Moon, R.; Roitman, D.; Stocking, A. *Science* **1996**, *273*, 884−888.

(24) Gymer, R. W. *Endeavour* **1996**, *20*, 115−120.

(25) Chang, S.-C.; Li, Y.; Yang, Y. *Polym. Mater. Sci. Eng.* **2001**, *84*, 1085−1086.

(26) Chang, S.-C.; Yang, Y. *Appl. Phys. Lett.* **1999**, *75*, 2713−2715.

(27) Chang, S.-C.; Yang, Y. *Polym. News* **2000**, *25*, 401−404.

(28) Yang, C.; He, G.; Wang, R.; Li, Y. *J. Appl. Polym. Sci.* **1999**, *73*, 2535−2539.

(29) Yang, Y.; Pei, Q.; Heeger, A. J. *J. Appl. Phys.* **1996**, *79*, 934−939.

(30) Peng, Z.; Zhang, J.; Xu, B. *Macromol.* **1999**, *32*, 5162−5164.

(31) Sun, Q.; Deng, Y.; Chen, J.; Tang, B. Z. *Europ. Polym. J.* **2005**, *41*, 481−489.

(32) Nicholson, R. S.; Shain, I. *Anal. Chem.* **1964**, *36*, 706−723.

(33) Bond, A. M. *Analyst* **1994**, *119*, R1−R21.

(34) Miao, W.; Bard, A. J. *Anal. Chem.* **2004**, *76*, 5379−5386.

(35) Bond, A. M.; Feldberg, S. W.; Miao, W.; Oldham, K. B.; Raston, C. L. *J. Electroanal. Chem.* **2001**, *501*, 22−32.

(36) Miao, W.; Choi, J.-P. In *Electrogenerated Chemiluminescence*; Bard, A. J., Ed.; Marcel Dekker: New York, 2004, Chapter 5.

(37) Lai, R. Y.; Bard, A. J. *J. Phys. Chem. A* **2003**, *107*, 3335−3340.